Effect of Dielectric Constant on the Zeta Potential of Spherical Electric Double Layers

Khawla Qamhieh *

Posted Date: 1 April 2024

doi: 10.20944/preprints202404.0012.v1

Keywords: Colloidal particles; Zeta potential; Monte Carlo; dielectric constant; charge inversion

 doi:10.20944/preprints202404.0012.v1

Article

Effect of Dielectric Constant on the Zeta Potential of Spherical Electric Double Layers

Khawla Qamhieh

Department of Physics, College of Science and Technology, Al-Quds University, Jerusalem, Palestine; khawlaq@gmail.com

Abstract: Zeta potential refers to the electrokinetic potential present in colloidal systems, exerting significant influence on the diverse properties of nano-drug delivery systems. The impact of dielectric constant on the zeta potential and charge inversion of highly charged colloidal particles, immersed in a variety of solvents spanning from polar, such as water, to nonpolar solvents, and in the presence of multivalent salts, was investigated through primitive model Monte Carlo (MC) simulations. Zeta potential ξ is decreased as decreasing the dielectric constant of the solvent, and upon further increase in the salinity and the valency of the salt. At elevated levels of salt, the colloidal particles become overcharged, in all solvents. As a result, their apparent charge becomes opposite in sign to the stoichiometric charge. This reversal of charge intensifies until reaching a saturation point with further increase in salinity, as a result, their apparent charge becomes opposite in sign to the stoichiometric charge. This reversal of charge intensifies until reaching a saturation point with further increase in salinity.

Keywords: colloidal particles; zeta potential; Monte Carlo; dielectric constant; charge inversion

1. Introduction

Charged colloids dispersed in solution are prevalent in both biological and technical systems. Examples include proteins, micelles, microemulsions, latex particles based on polystyrene, and silica particles. Physiochemical properties of these systems are controlled to a large degree by electrostatic interactions [1]. In an electrolyte solution, a charged colloidal particle is typically surrounded by small ions of opposite charge, known as counterions, which serve to balance the surface charge. The charged surface of the colloidal particle, along with the surrounding diffuse layer of ions, is commonly referred to as the electric double layer (EDL). This EDL plays a fundamental role in the stability and coagulation of dispersed systems, as described by DLVO theory [2,3]. EDL could have different geometry such as planar [4], cylindrical [1], spherical [5], and ellipsoidal [6] depending on the charged surface geometry. Due to its widespread presence in both natural and technological realms, this phenomenon has garnered significant attention from the scientific community. It encompasses a wide range of engineering applications including colloid stability, energy conversion, desalination, separation processes, nanofabrication, nanofluidic devices, and ion transport across membranes [7-9].

The electrostatic correlations among ions within the electric double layer (EDL) can give rise to a range of intriguing phenomena in systems containing multivalent ions. These may include phenomena such as charge inversion or short-range attraction between macroions of like charge. These correlations have been neglected in the DLVO theory through applying the mean field approaches [1,5,10-13].

Computer simulations and theoretical investigations have demonstrated that correlation-induced attraction or charge inversion can serve as a driving force for the aggregation of colloidal particles, even in the presence of small multivalent ions [14-17]. The universality of the implicit phenomena is understood to stem from the significant energetic contribution of Coulombic interactions to the free energy, which surpasses that of entropy and renders the system relatively insensitive to the internal structure of the counterions [16,18,19]. Martin-Molina and colleagues

 doi:10.20944/preprints202404.0012.v1

investigated the charge inversion of colloids in electrolyte mixtures comprising both multi- and monovalent counterions [20]. They demonstrate that incorporating short-term correlations between ions into the study of ion distribution yields markedly different results from classical treatments. In their study, charge inversion was observed in the presence of an electrolyte mixture containing both multi- and monovalent counterions. EDL properties can be affected by many factors, for examples are the excluded volume of small ions [21,22], and the asymmetry in electrolyte valence [23]. Schwer and Kenndler conducted experimental research on the impact of solvent composition's dielectric constant on electroosmotic flow in fused-silica capillaries. They concluded that, except for acetone-water mixtures, increasing the fraction of organic solvent in water led to a decrease in Zeta potential [24].

In our investigation, we utilized Monte Carlo (MC) simulations to explore the properties of spherical electric double layers (EDLs) surrounding highly charged colloidal particles immersed in various solvents, ranging from polar solvents like water to nonpolar ones. Our aim was to examine the influence of dielectric constant on the zeta potential and charge inversion of colloidal particles in the presence of multivalent salts, including trivalent and pentavalent ions. The study of spherical EDLs is particularly pertinent due to their significance in dispersions of globular proteins, micelles, polymer beads, dendrimers, and other closely spherical organic or inorganic macroions [23]. The structure of the article is outlined as follows: Section 2 provides details on the model and parameters settings used for the numerical calculations. Section 3 presents the results and discussion derived from the simulations conducted. The conclusions are outlined in the fourth section.

2. Model and Method

2.1. Model

The macroion is represented as a hard sphere of radius R_M = 20 Å, and has a charge of valence Z_M = -60, impeded at the center of spherical cell of radius 100 Å, including asymmetric electrolytes described within the scope of the primitive model, whereas the solvent enters the model by its dielectric constant ϵ_r. The dielectric constants and the corresponding Bjerrum lengths for the solvents used in our study are shown in Table 1. The electrolyte also contains small ions of radius R_I = 2 Å, and charge valence Z_I = +1, representing the counterions, while the solvents enter by its dielectric constant. The added salt consists of small ions of radius 2 Å, monovalent anions Z_a = -1 and cations of different valencies, trivalent ones Z_c = +3, and pentavalent cations Z_c = +5. The amount of added salt is characterized by the ratio of the total added cation charge to the total macroion charge, $\beta = Z_c \rho_c/(Z_M \rho_M)$, where ρ_c is the number density of the corresponding species. In the study many values of β between 0.15 to 8 are used. The systems are considered at a macroion number density, $\rho_M = 2.5 * 10^{-7}$ Å^{-3} related to a macroion volume fraction $\emptyset_M = 0.008$, keeping the temperature constant at $T = 298$ K. In our model the electrostatic interaction between the particles is pairwise additive, and for pair *ij* it is given by

$$U_{ij}(r) = \begin{cases} \infty, r_{ij} < (R_i + R_j) \\ \dfrac{Z_i Z_j e^2}{4\pi\varepsilon_0\varepsilon_r}\dfrac{1}{r_{ij}}, r_{ij} \geq (R_i + R_j) \end{cases} \quad eq.1$$

where i and j denote either polyion or counterion. The intensity of the electrostatic correlations between counterions on the surface can be characterized by the counterion-counterion coupling parameter $\Gamma = Z_I^2 l_b/a_Z$ and can be increased by lowering the solvent dielectric constant, $l_b = e^2/4\pi\varepsilon_0\varepsilon_r k_B T$ is the Bjerrum length, where e is the elementary charge, k_B is Boltzman constant, and T is the temperature in kelvin, and $a_Z = [Z_I/(\sigma/e)]^{1/2}$ is the average distance between two neighboring counterions on a surface has σ surface charge density, and it is known that the correlation-induced attraction appears at $\Gamma > \Gamma^* \approx 2$ [13,25]. The dielectric constants, the Bjerrum lengths for the solvents used in our study and the corresponding Coulomb coupling parameters (Γ) between monovalent, trivalent, and pentavalent counterions on the charged surface in all solvents are shown in Table 1, which illustrates increment in the counterion-counterion coupling parameter Γ, meaning an increment in the intensity of the electrostatic correlations between counterions on the

 doi:10.20944/preprints202404.0012.v1

surface of the macroion, as the valence of the counterion is increased, and the dielectric constant of the solvent ε_r is decreased.

Table 1. Dielectric constants ε, Bjerrum lengths for the solvents used, and the corresponding Counterion - counterion coupling parameter (Γ) between the monovalent, trivalent, and pentavalent counterions on the charged surface in all solvents used in our study.

The solvent	Water	(75%water, 25% ethanol)	Methyl alcohol	Glycerin	Methanol	Ethanol
Dielecrtiric constant (ε)	78	68	54	40	30	20
l_B (Å)	7.1	8.2	10.4	14.0	18.7	28.0
Γ_1	0.8	0.9	1.1	1.5	2.0	3.0
Γ_3	4.1	4.7	5.7	7.8	10.4	15.6
Γ_5	8.9	10.1	12.3	16.8	22.4	33.5

2.2. Method and Simulation Settings

In our study, Monte Carlo (MC) simulation method was applied and employed the canonical *NVT* ensemble with periodic boundary conditions and the Ewald summation for treating the electrostatic interactions. We performed 10^6 MC moves per particles in the production run, while for systems at β = 6.25 we performed up to 10^5 moves. The macroion is fixed at the center of a spherical cell, while the small ions were initially placed randomly inside it. The simulation software MOLSIM v3.1, developed by Per Linse and colleagues, was utilized in this study. Additional information regarding the simulation methodology can be found in reference [26].

3. Results and Discussion

3.1. Systems Without Salts:

Figure 1 illustrates the macroion-counterion radial distribution functions (rdf's), describing the relative densities of counterions at a distance r from the macroion for the 60:1 system in different solvents, with different dielectric constants as in Table 1. The horizontal dotted line exemplifies systems of uncorrelated particles. The figure shows a maxima at the hard sphere contact separation r = R_M + R_I = 22 Å for the macroion-counterion rdf's curves demonstrating the accumulation of the counterions close to the macroion. At ε = 20, where $\Gamma = 3$, the value of the maximum is 505 and decreases monotonically as the dielectric constant of the solvent is increased and gives a value of 120 at ε = 78 where $\Gamma = 0.8$, meaning the maximum is decreased as the electrostatic intensity is decreased.

Preprints.org (www.preprints.org) | NOT PEER-REVIEWED | Posted: 1 April 2024 doi:10.20944/preprints202404.0012.v1

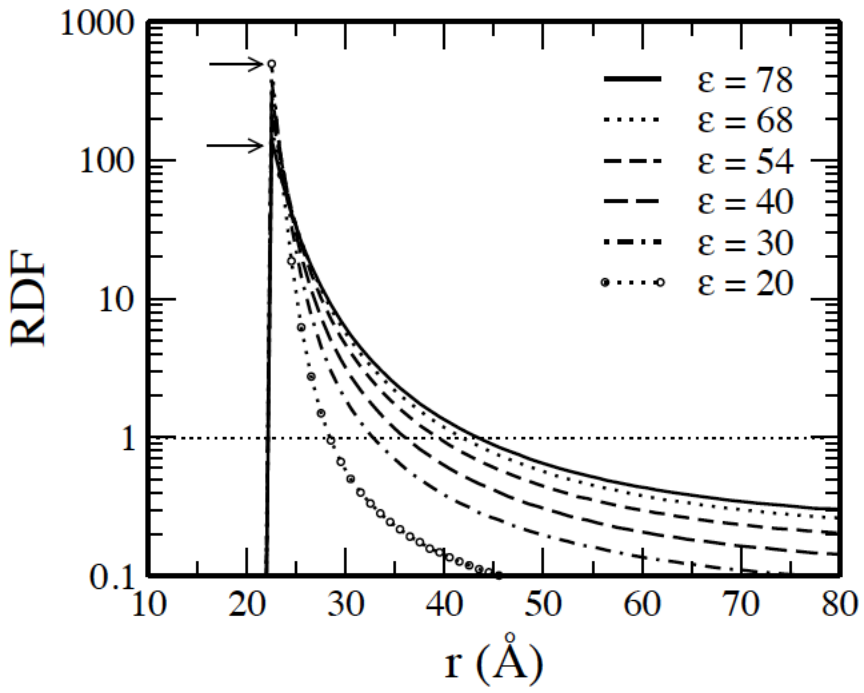

Figure 1. Macroion-counterion radial distribution functions for 60:1 system, at indicated values of the dielectric constants ε. The arrows point on the values at $r = R_M + R_I = 22$ Å. The dotted horizontal line represents at g_{MI} corresponds to uncorrelated particles in the systems.

The accumulated running charge Z_{acc}(r), within a distance r from the center of the macroion, is an important quantity that follows directly from the macroion-ion radial distribution function g_{MI} according to

$$Z_{acc}(r) = Z_M + \int_r^{\infty} \sum [Z_i \rho_i g_{Mi}(r')] 4\pi r'^2 dr' \quad eq.2$$

where ρ_i is the uniform number density of the corresponding species. The accumulated running charge can be used to calculate the mean electrostatic potential at a distance r from the center of the macroion, where

$$\varphi(\mathrm{r}) = \int_r^{\infty} dr' E(r') = \frac{e}{4\pi\varepsilon'} \int_r^{\infty} dr' \frac{Z_{acc}(r')}{r'^2} \quad eq.3$$

The upper cutoff in eq. 3 is taken to be 60 Å since the typical accumulated charge rabidly decays to zero [27]. The surface potential φ_s is the electric potential at the surface of the macroion i.e., $\varphi_s = \varphi(R_M)$, while the zeta potential ξ is identified with the diffuse potential at the slipping plane or hydrodynamic shear surrounding a particle surface and located at one ionic diameter away from the macroion i.e., $\xi = \varphi(R_M + 2R_I)$.

The accumulated running charge curves are presented in Figure 3a, which shows that the total charge decays monotonically and reaches zero at the cell boundary in all systems, and the decay rate increases by changing the solvent from water as a polar solvent to nonpolar ones, means decreasing the dielectric constant. This can be explained by the escalation in the counterion-counterion coupling parameter Γ as the dielectric constant of the solvent is decreased as shown in Table 1. The negative value of the mean electrostatic potential $\varphi(r)$ of the macroion *EDL*, shown in Figure 3b, is rabidly decreased when the polarity of the solvent is decreased, as a consequence of decreasing the effective charge of the macroion Z_M^{eff} by decreasing the dielectric constant as illustrated in Figure 4, where $Z_M^{eff} = Z_{acc}(R+2R_I)$. The value of Z_M^{eff} starts from about 0.54 Z_M at ε = 78.4 with water solvent and then decreases to reach 0.07 Z_M at the lowest dielectric constant ε = 20

Preprints.org (www.preprints.org) | NOT PEER-REVIEWED | Posted: 1 April 2024 doi:10.20944/preprints202404.0012.v1

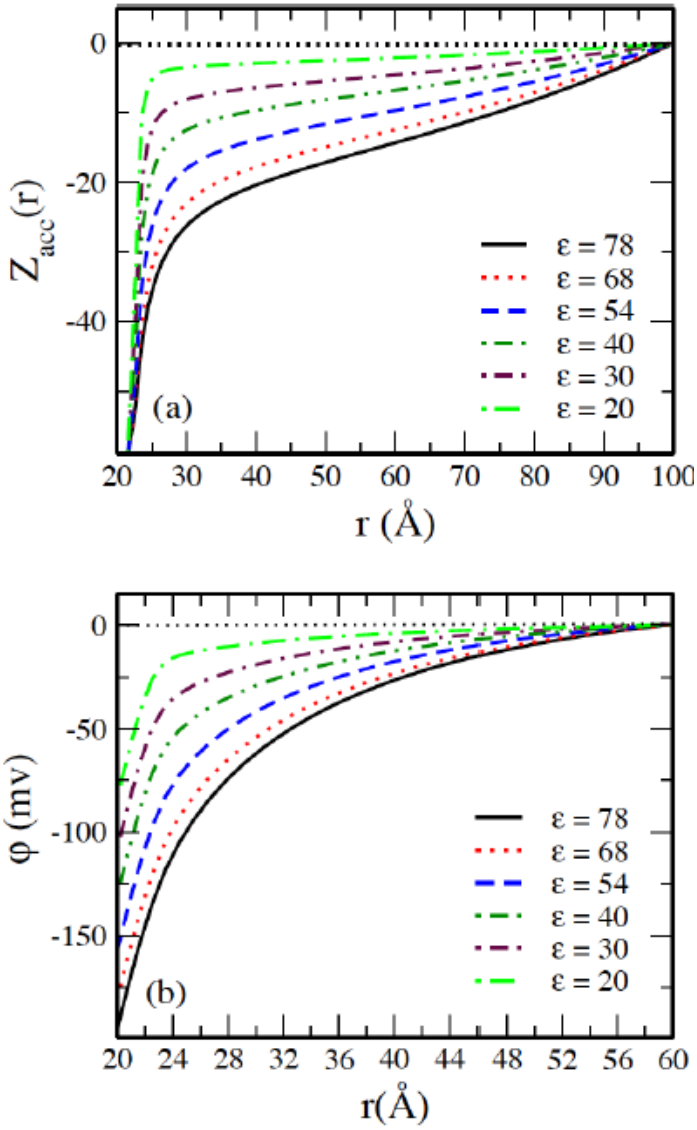

Figure 3. a) Accumulated running charge Z_{acc} (r), and b) mean electrostatic potential $\varphi(r)$ of the macroion EDL as a function of distance r from the macroion center for 60:1 system in solvents with the indicated dielectric constants ε.

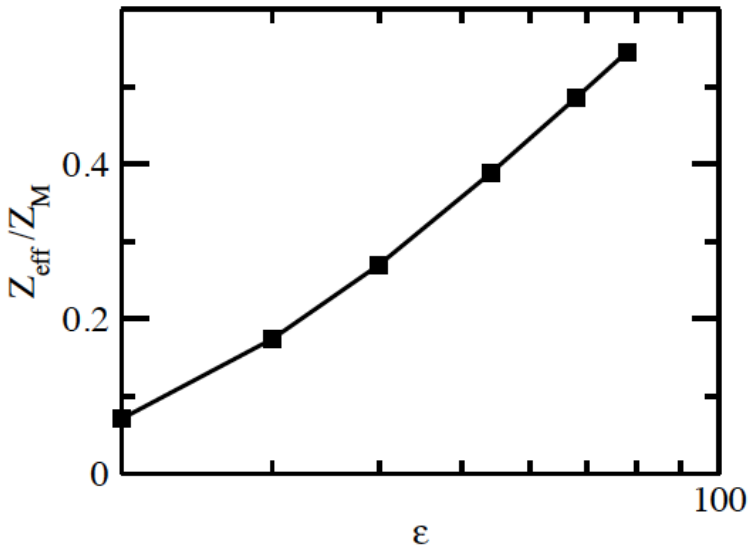

 doi:10.20944/preprints202404.0012.v1

Figure 4. Effective macroion charge for 60:1 system in different solvents as a function of the dielectric constant ε.

Figure 5 shows that the negative values of the surface φ_s, and the ξ potentials are linearly decreased by decreasing the dielectric constant. Our finding for ξ potential is in good agreement with the experimental result concluded by Schower et al. [24], where they found that ξ potential is decreased as the fraction of organic solvent in water is increased, i.e., decreasing the polarity of the solvent and consequently the dielectric constant of the solvent is decreased.

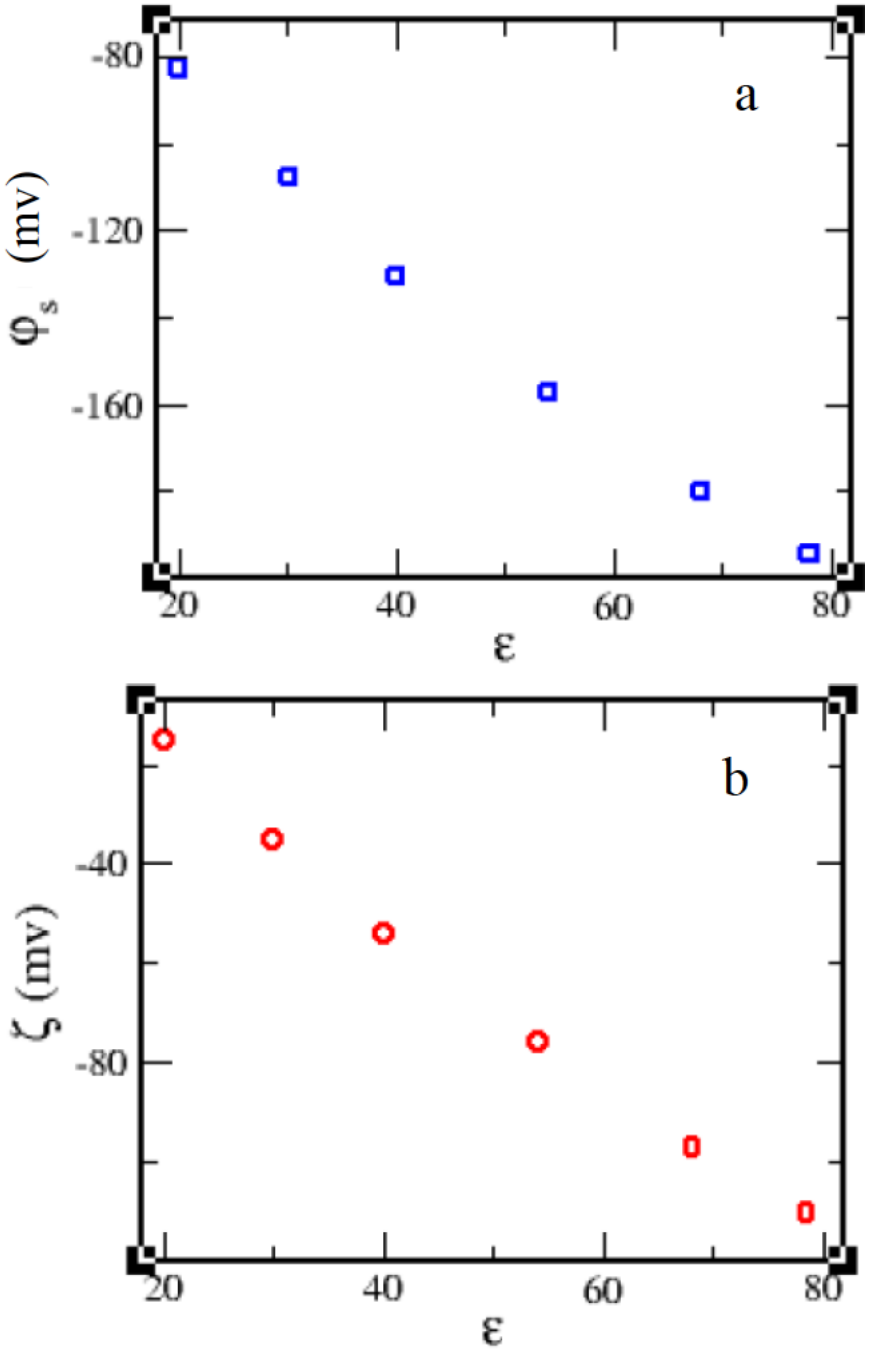

Figure 5. a) Zeta potential ξ, and b) surface potential φ_s of *EDL* as a function of ε for 60:1 system in different solvents without salt.

The decrement in ξ potential is a natural result of the greater accumulation of the counterions around the macroion with smaller dielectric constant than it is with greater ones as it is clear in Figure 6, which illustrates snapshots for the distribution of the counterions around the macroion for 60:1

 doi:10.20944/preprints202404.0012.v1

system in solvents with different dielectric constants. The greater accumulation of the counterions around the macroion leads to a decrease in the effective charge of the macroion Z_M^{eff} on which ξ potential depends.

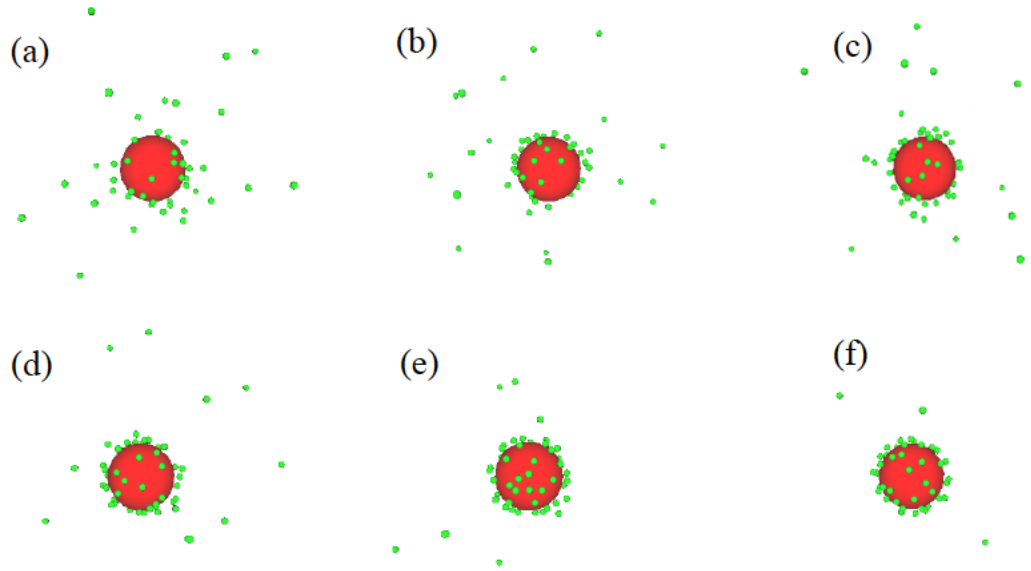

Figure 6. Counterions (green, small balls) distribution around the macroion (red large ball) for 60:1 system in solvents with different dielectric constants, a) ε = 78, b) ε = 68, c) ε = 54, and d) ε = 40, f) ε = 30, g) ε = 20.

3.2. Systems with Salt

Figure 7 shows the accumulated running charge $Z_{acc}(r)$ as a function of the distance r from the center of the macroion for the 60:1 system in solvents with different dielectric constants at different 3:1 salt concentration. There is a distinct qualitative difference between the systems as the salt concentration is increased. At low salt concentration β = 0.15, the total charge decays monotonically and reaches zero only at the cell boundary in all systems and the decay rate increases by decreasing the polarity of the solvent means the dielectric constant is decreased as shown in Figure 7a. At higher salt concentrations the charge shows a sharp drop to zero within a very narrow region r < 48 Å. At β = 1, Z_{acc} (r) shown in Figure 7b remains close to zero up to the cell boundary in solvents with relatively high dielectric constant like water. In solvents with lower dielectric constants the charge changes its sign reaches a maximum and then decays slowly, similar to what occurs for the charges in systems with higher salt concentration β =6.25 shown in Figure 7c. The figure shows a maximum of charge equals to ≈+34 at ε = 20 and decreases monotonically as the dielectric constant of the solvent is increased and gives a value of ≈+7 at ε = 78. Close to the cell boundary the figure shows a build up in the cation charge, as a result of the repulsion between the charge inverted macroions and the cations.

Preprints.org (www.preprints.org) | NOT PEER-REVIEWED | Posted: 1 April 2024 doi:10.20944/preprints202404.0012.v1

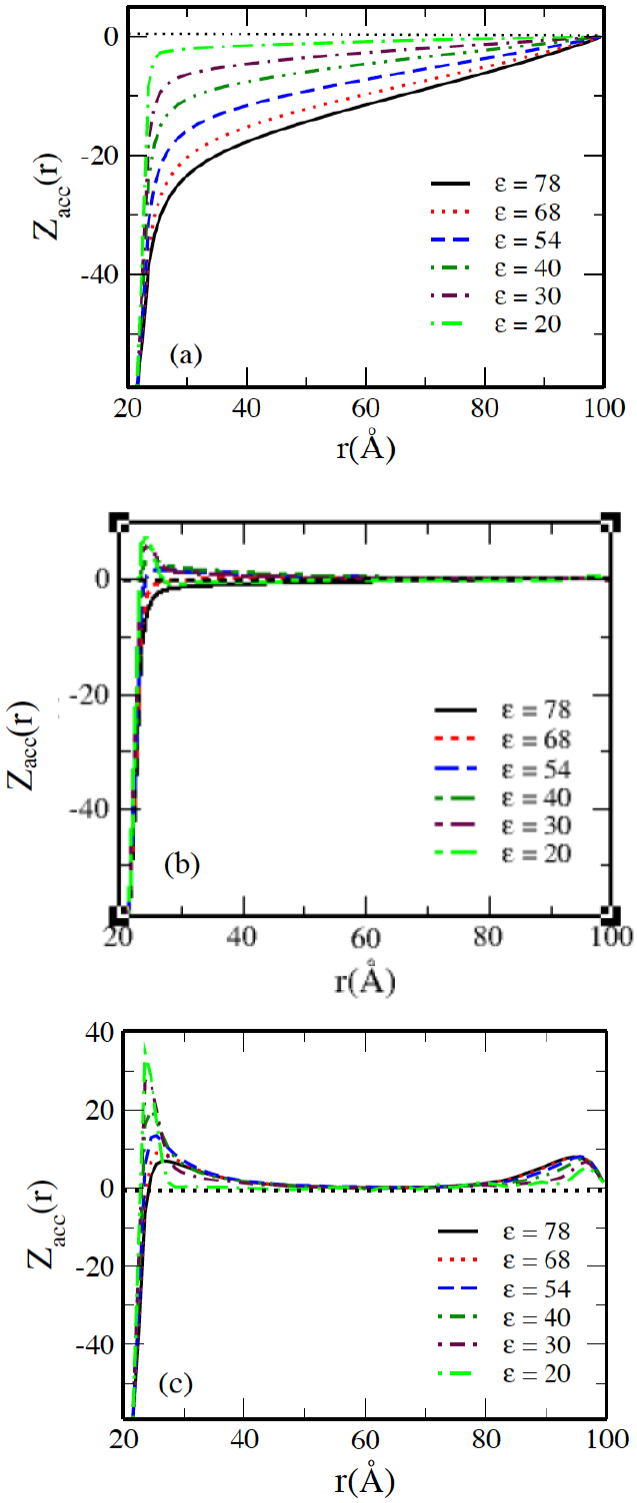

Figure 7. Accumulated running charge $Z_{acc}(r)$ as a function of the distance r from the macroion center in solvents with the indicated dielectric constants ε and salt concentration of a) β = 0.15, b) β = 1, c) β = 6.25.

Figure 8 illustrates surface electrostatic potential φ_s, and zeta potential ξ of EDL as a function of ε for 60:1 system in different solvents at different 3:1 and 5:1 salt concentrations as indicated in the figure. The decrease in the absolute values of these potentials is almost linear when ε is changed from 20 to 78, which is a consequence of the decrease in the intensity of the electrostatic correlations between counterions on the surface of the macroion.

Preprints.org (www.preprints.org) | NOT PEER-REVIEWED | Posted: 1 April 2024 doi:10.20944/preprints202404.0012.v1

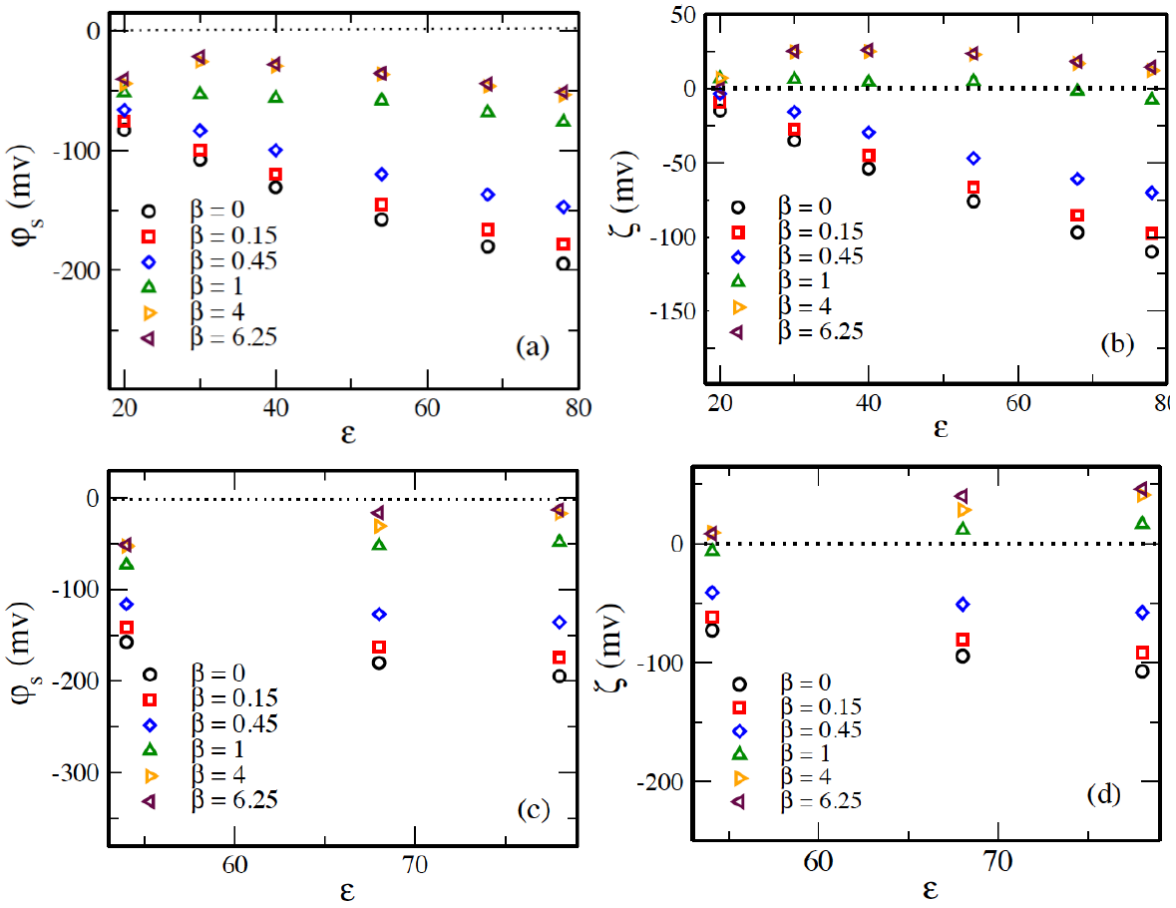

Figure 8. (a), (c) Surface electrostatic potential φ_s, and (b), (d) zeta potential ξ of EDL as a function of ε for 60:1 system, in different solvents at different (a), (b) 3:1, and (c), (d) 5:1 salt concentrations as indicated in the figures.

The values of φ_s and ξ potentials at $\beta = 4$ is very close to those at $\beta = 6.25$, and the potentials at $\beta = 0$, $\beta = 0.15$, and $\beta = 0.45$ are much less negative than those at $\beta < 1$. At $\beta = 1$, ξ potential is close to zero corresponding to neutralized macroion while its values inverted to positive with salt concentrations $\beta > 1$ where charge inversion occurs. The decrease in the potential by changing salt concentration, is largest when $\varepsilon = 78$, while it is smallest when $\varepsilon = 20$. The decrease is larger in the systems with 5:1 salt, where ξ is changed from $\approx$-110 mv to $\approx$+45 mv at $\varepsilon = 78$, while it is changed to $\approx$+13 mv in the systems with 3:1 salt, means that charge inversion is larger with 5:1 salt than it is with 3:1 salt as the coupling parameters are larger in systems with 5:1 salt.

In Figure 9 we plotted the reduced electrostatic energy of the solution U/Nk_BT for the 60:1 system once with 3:1 (Figure 9a) and another with 5:1 salt concentration (Figure 9b) in different solvents with different dielectric constants, where N is the total number of the ionic species. Figure 9 shows that the total potential energy is negative in all systems because of strong attraction between the macroion and counterions. Its magnitude decreases monotonically with the salt content, which is a simple consequence of increasing the overall number of particles, and is more negative with 5:1 salt than with 3:1 salt at specific salt concentration. All the curves have similar shapes with varying curvatures. An inflection point is observed at about $\beta = 1$ on each curve. The decrease in the magnitude is smaller with 5:1 salt than with 3:1 salt.

 doi:10.20944/preprints202404.0012.v1

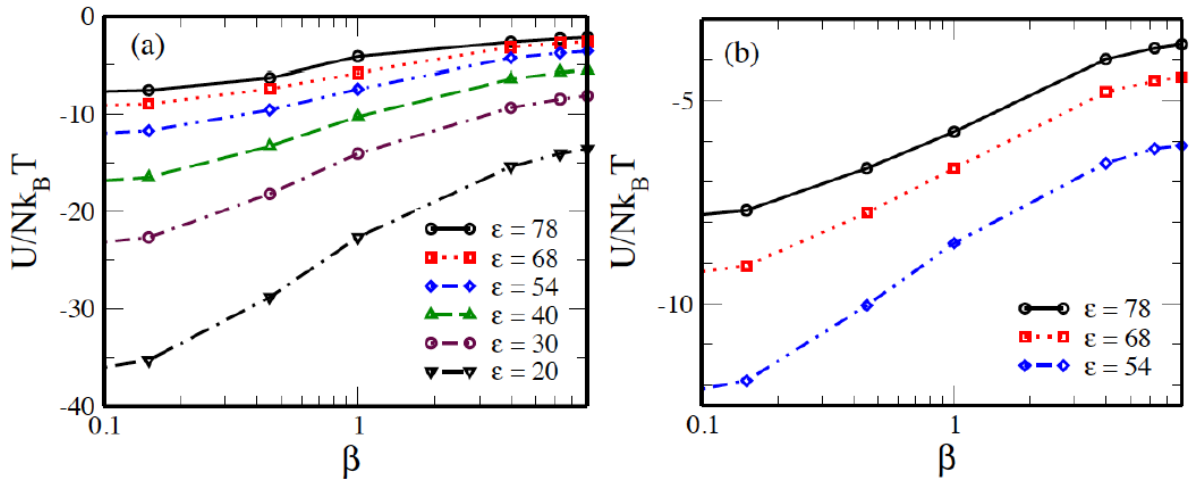

Figure 9. Reduced electrostatic energy as a function of (a) 3:1 and (b) 5:1 salt concentration β, for 60:1 system in different solvents with different dielectric constants ε as indicated in the figure.

In Figure 9, we illustrate the reduced electrostatic energy of the solution U/Nk_BT for the 60:1 system, once with a 3:1 salt concentration (Figure 9a) and another with a 5:1 salt concentration (Figure 9b), in various solvents with differing dielectric constants, where N represents the total number of ionic species. Figure 9 demonstrates that the total potential energy is consistently negative across all systems due to the strong attraction between the macroion and counterions. This energy decreases monotonically with the salt content, reflecting the simple consequence of an increasing overall number of particles, and is more negative with 5:1 salt concentration compared to 3:1 salt concentration at specific salt concentrations. All curves exhibit similar shapes with varying curvatures, with an observed inflection point at approximately $\beta = 1$ on each curve. The reduction in magnitude is less pronounced with 5:1 salt concentration than with 3:1 salt concentration.

4. Conclusions

We performed a numerical investigation on electrolyte solutions with significant asymmetry, comprising highly charged colloidal particles in different solvents, once, without salt, and another in different amounts of multivalent salt. Decreasing the polarity of the solvent without salt, means deceasing ε, gradually lowers the effective charge, the surface potential φ_s, and the zeta potential of the colloidal particles. Addition of minute quantities of multivalent salt yields a similar effect in all solvents. When the dosage of multivalent salt surpasses the macroion's isoelectric concentration, it induces charge inversion in the macroion. This reversed charge escalates to a saturation point with continued salinity increase.

Currently, colloidal nano-carriers are undergoing rapid growth owing to their considerable potential in resolving persistent challenges like poor drug solubility and bioavailability. Moreover, they exhibit limitless possibilities in drug targeting. Our findings hold immense significance, as the properties of nano-medicines, including their release from dosage forms at specific sites, as well as drug circulation and absorption into bodily membranes, are significantly affected by the zeta potential (ξ) of nano-drugs [28].

References

1. Qamhieh, K.; Linse, P. Effect of Discrete Macroion Charge Distributions in Solutions of Like-Charged Macroions. *Journal of Chemical Physics* **2005**, *123* (10), 104901-104912. https://doi.org/10.1063/1.1979496.
2. Gonzclez-Tovar, E.; Lozada-Cassou, M. *The Spherical Double Layer: A Hypernetted Chain Mean Spherical Approximation Calculation for a Model Spherical Colloid Particle*; 1989; Vol. 93, 3761-3768.
3. Verway, E. J.; Overbeek, I. Th. G. *Theory of the Stability of Lyophobic Colloid*; Elsevier: New York, 1948.

4. Yang, K.; Yiacoumi, S.; physics, C. T.-T. J. of chemical; 2002, undefined. Monte Carlo Simulations of Electrical Double-Layer Formation in Nanopores. *aip.scitation.org* **2002**, *117* (18), 8499–8507. https://doi.org/10.1063/1.1511726.
5. Qamhieh, K.; Amleh, M.; Khaleel, M. Effect of Discrete Macroion Charge Distributions on Electric Double Layer of a Spherical Macroion. *J Dispers Sci Technol* **2013**, *34* (11), 1517–1525. https://doi.org/10.1080/01932691.2012.751878.
6. Bulavchenko, A. I.; Batishchev, A. F.; Batishcheva, E. K.; Torgov, V. G. Modeling of the Electrostatic Interaction of Ions in Dry, Isolated Micelles of AOT by the Method of Direct Optimization. *ACS Publications* **2002**, *106* (25), 6381–6389. https://doi.org/10.1021/jp0144000.
7. Zhang, L.; Hesse, M.; Electrophoresis, M. W.-; 2019, undefined. Dispersion of Charged Solute in Charged Micro-and Nanochannel with Reversible Sorption. *Wiley Online Library* **2019**, *40* (6), 838–844. https://doi.org/10.1002/elps.201800334.
8. Li, S. X.; Guan, W.; Weiner, B.; Reed, M. A. Direct Observation of Charge Inversion in Divalent Nanofluidic Devices. *Nano Lett* **2015**, *15* (8), 5046–5051. https://doi.org/10.1021/ACS.NANOLETT.5B01115.
9. Cao, L.; Ma, W.; Zhu, D. B.; Guo, W.; Xia, J.; Nie, F.-Q.; Xue, J.; Song, Y.; Zhu, D.; Wang, Y.; Jiang, L. Energy Harvesting with Single-ion-selective Nanopores: A Concentration-gradient-driven Nanofluidic Power Source. *Wiley Online Library* **2010**, *20* (8), 1339–1344. https://doi.org/10.1002/adfm.200902312.
10. Qamhieh, K.; Nylander, T.; Black, C. F.; Attard, G. S.; Dias, R. S.; Ainalem, M. L. Complexes Formed between DNA and Poly(Amido Amine) Dendrimers of Different Generations-Modelling DNA Wrapping and Penetration. *Physical Chemistry Chemical Physics* **2014**, *16* (26), 13112–13122. https://doi.org/10.1039/c4cp01958j.
11. Qamhieh, K.; Khaleel, A. A. Analytical Model Study of Complexation of Dendrimer as an Ion Penetrable Sphere with DNA. *Colloids Surf A Physicochem Eng Asp* **2014**, *442*, 191–198. https://doi.org/10.1016/j.colsurfa.2013.01.047.
12. Qamhieh, K.; Nylander, T.; Ainalem, M. L. Analytical Model Study of Dendrimer/DNA Complexes. *Biomacromolecules* **2009**, *10* (7), 1720–1726. https://doi.org/10.1021/bm9000662.
13. Lobaskin, V.; Qamhieh, K. Effective Macroion Charge and Stability of Highly Asymmetric Electrolytes at Various Salt Conditions. **2003**, 107 (32), 8022-8029.https://doi.org/10.1021/jp027608.
14. Lin, C.; Qiang, X.; Dong, H. L.; Huo, J.; Tan, Z. J. Multivalent Ion-Mediated Attraction between Like-Charged Colloidal Particles: Nonmonotonic Dependence on the Particle Charge. *ACS Omega* **2021**, *6* (14), 9876–9886. https://doi.org/10.1021/acsomega.1c00613.
15. Linse, P.; letters, V. L.-P. review; 1999, undefined. Electrostatic Attraction and Phase Separation in Solutions of Like-Charged Colloidal Particles. *APS* **1999**, *83* (20), 4208–4211. https://doi.org/10.1103/PhysRevLett.83.4208.
16. Shklovskii, B. I. Wigner Crystal Model of Counterion Induced Bundle Formation of Rodlike Polyelectrolytes. *Phys Rev Lett* **1999**, *82* (16), 3268–3271. https://doi.org/10.1103/PHYSREVLETT.82.3268.
17. Linse, P. Mean Force between Like-Charged Macroions at High Electrostatic Coupling. *J. Phys.: Condens. Matter* **2002**, *14*, 13449–13467.
18. Carlsson, F.; Malmsten, M.; Linse, P. Protein-Polyelectrolyte Cluster Formation and Redissolution: A Monte Carlo Study. *J Am Chem Soc* **2003**, *125* (10), 3140–3149. https://doi.org/10.1021/JA020935A.
19. Skepö, M.; Linse, P. Complexation, Phase Separation, and Redissolution in Polyelectrolyte - Macroion Solutions. *Macromolecules* **2003**, *36* (2), 508–519. https://doi.org/10.1021/MA020634L.
20. 20 Martín-Molina, A.; Quesada-Pérez, M.; Galisteo-González, F.; Hidalgo-' Alvarez, R. *Probing* Charge Inversion in Model Colloids: Electrolyte Mixtures of Multi-and Monovalent Counterions *J. Phys.: Condence. Matter* **2003**,15, S3475-S3483.
21. Messina, R.; Holm, C.; Kremer, K. Effect of Colloidal Charge Discretization in the Primitive Model. *European Physical Journal E* **2001**, *4* (3), 363–370. https://doi.org/10.1007/S101890170119.
22. Besteman, K.; Zevenbergen, M. A. G.; Lemay, S. G. Charge Inversion by Multivalent Ions: Dependence on Dielectric Constant and Surface-Charge Density. *Phys Rev E Stat Nonlin Soft Matter Phys* **2005**, *72* (6), 061501-061509. https://doi.org/10.1103/PhysRevE.72.061501.
23. Guerrero-García, G. I.; González-Tovar, E.; Lozada-Cassou, M.; Guevara-Rodríguez, F. D. J. The Electrical Double Layer for a Fully Asymmetric Electrolyte around a Spherical Colloid: An Integral Equation Study. *Journal of Chemical Physics* **2005**, *123* (3), 034703-034723. https://doi.org/10.1063/1.1949168.
24. Schwer, C.; Kenndler, E. Electrophoresis in Fused-Silica Capillaries: The Influence of Organic Solvents on the Electroosmotic Velocity and the ζ Potential. *Anal Chem* **1991**, *63* (17), 1801–1807. https://doi.org/10.1021/ac00017a026.
25. Rouzina, I.; Bloomfield, V. A. Macroion Attraction Due to Electrostatic Correlation between Screening Counterions. 1. Mobile Surface-Adsorbed Ions and Diffuse Ion Cloud. *Article in The Journal of Physical Chemistry* **1996**, 100 (23), 9977-9989. https://doi.org/10.1021/jp960458g.

 doi:10.20944/preprints202404.0012.v1

26. Lobaskin, V.; Linse, P. Simulation of an Asymmetric Electrolyte with Charge Asymmetry 60:1 Using Hard-Sphere and Soft-Sphere Models. Journal of chemical physics 1999, 111 (9), 4300-4309. http://ojps.aip.org/jcpo/jcpcpyrts.html.
27. Diehl, A.; Levin, Y. Smoluchowski Equation and the Colloidal Charge Reversal. *Journal of Chemical Physics* **2006**, *125* (5). 054902-054906. https://doi.org/10.1063/1.2222372.
28. Honary, S.; research, F. Z.-T. journal of pharmaceutical; 2013, undefined. Effect of Zeta Potential on the Properties of Nano-Drug Delivery Systems-a Review (Part 1). *ajol.infoS Honary, F ZahirTropical journal of pharmaceutical research, 2013•ajol.info* **2013**, *12* (2), 255–264. https://doi.org/10.4314/tjpr.v12i2.19.